

Technical Note

Periodic structures of randomly distributed Cu/Cu₂O nanograins and periodic variations of cell voltage in copper electrodeposition

M.-Z. Zhang^{a,*}, M. Wang^{a,b}, Z. Zhang^c, J.-M. Zhu^a, R.-W. Peng^a, N.-B. Ming^a

^a National Laboratory of Solid State Microstructures and Department of Physics, Nanjing University, Nanjing 210093, China

^b International Center of Quantum Structures, Institute of Physics, Chinese Academy of Sciences, Beijing 10080, China

^c Institute of Physics, Chinese Academy of Sciences, Beijing 10080, China

Received 17 March 2003; received in revised form 22 December 2003; accepted 2 January 2004

Abstract

Copper electrodeposition can create periodic self-assembled structures with randomly distributed Cu/Cu₂O nanograins and spontaneously periodic variations of cell voltage in the presence of an ultrathin layer of concentrated CuSO₄ electrolyte. The experiment was performed at -4.85°C and cell currents of $30\ \mu\text{A}$. We suggest that the observed self-assembled structures and periodic variations of cell voltage are caused by a change in the cathode over-potential and the standard electrode potential for Cu₂O and Cu in front of the growing interface. The mechanism of the self-assembled structure and the spontaneously periodic variations of cell voltage is discussed.

© 2004 Elsevier Ltd. All rights reserved.

Keywords: Copper electrodeposition; Self-assembly; Nanograins; Cathode over-potential; Electrode potential

1. Introduction

The importance of copper for next-generation on-chip interconnection has been well established since the first discovery that copper wiring has advantages of lower resistance, higher allowable current density, and increased scalability compared with the Ti/Al (Cu) wiring [1,2]. Much effort has been devoted to copper electrodeposition in recent years because of the technological requirements and scientific interests [3–10].

The growth of branched metal aggregates by electrochemical deposition in quasi-two-dimensional geometries is a complex example of nonequilibrium growth [5–7]. In the thin-layer electrochemical deposition of CuSO₄, a variety of different growth morphologies have been observed depending on the experimental conditions in the quasi-two-dimensionality [5–18]. Electrochemical deposition processes occurring at the interface is determined by diffusion, migration, convection, and chemical processes [5]. To understand and control the deposit formation, it is important to know the various electrochemical and physi-

cal processes near the growing interface, for instance, the effect of the cathode over-potential and electrolyte ion electrode potential [12,19–27]. Ions drift in the applied electric field, and electrochemical reactions occur at both cathode and anode. The reactions lead to spatial variations in the concentration of ions near both electrodes and the variety of charge at the electrodes [3–10]. In addition, the change of the ion concentration at the electrodes depending on time can trigger new electrochemical reactions or lead to time dependence on the electrode processes [19]. The electrodeposition can be nucleation controlled [19,22], which is sensitive to the variation of concentration/electric fields at the growing front. These factors would induce oscillatory nucleation and growth, as well as copper/cuprous oxide resulting from nonequilibrium [11,19,22,28,29].

Recently, the electrodeposition of copper in an ultrathin layer of concentrated CuSO₄ electrolyte indicated that the macroscopic fingering branches of deposits consisting of long copper filaments covered with periodic corrugated nanostructures. The copper filaments deposited on an insulating glass substrate without introducing additives in the electrolyte or metallic clusters on the substrate surface. The investigation showed that electrolyte ion electrode potential influenced the formation of periodic structures [22,23].

* Corresponding author. Permanent address: Department of Materials Science & Engineering, Jilin University, Chang Chun 130025, China.

E-mail address: mzzhang@nju.edu.cn (M.-Z. Zhang).

However, nucleation sites of copper/cuprous oxide in quasi-two-dimensional electrochemical deposition have no direct experimental evidence. Also, the formation mechanism for an electrodeposited texture remains unclear. Therefore, it is interesting to explore self-assembled structures of copper/cuprous oxide in the copper electrodeposition.

In this paper, the electrodeposition with branched growth was observed on an insulating substrate using an ultrathin layer of concentrated CuSO_4 electrolyte. The copper electrodeposition can create periodic self-assembled structures along the branch with the random distribution of $\text{Cu}/\text{Cu}_2\text{O}$ nanograins and the spontaneously periodic variations of cell voltage. Phase composition, grain size, surface texture, and distribution of copper/cuprous oxide were investigated further by scanning electron microscopy (SEM), and high-resolution transmission electron microscopy (TEM). The formation mechanism of the self-assembled structure and the periodic variations of cell voltage was also discussed.

2. Experimental

The electrochemical cell for experiments consists of two clean cover glass plates. Separated by the electrodes, the cell gap is determined by the electrodes. Copper foil (99.9%) of thickness $40\ \mu\text{m}$ was generally used as spacers. The experiments were conducted in a cell enclosing two parallel electrodes separated by a distance of 8 mm. The electrolyte solution was prepared from analytical reagent CuSO_4 and ultrapure water. The concentration of CuSO_4 electrolyte is 0.05 M. A Peltier element and a temperature selector were employed to reduce temperature and to solidify the electrolyte. CuSO_4 is partially expelled from the solid in the solidification due to the partitioning effect. Eventually, an ultrathin layer of concentrated CuSO_4 electrolyte is formed between the ice of electrolyte solution and the upper/or the lower glass plate when equilibrium is reached. The layer thickness is about 200–400 nm and the concentration in this trapped layer does not exceed 0.7 M [22,23]. Experiments are carried out at $-4.85\ ^\circ\text{C}$. The electrodeposit develops in this layer. A constant Current of $30\ \mu\text{A}$ was applied. The deposited specimen was preserved with nitrogen for SEM and TEM observed.

Optical microscopy (OPM; Leitz, Orthoplan-pol) was employed in situ to observe the ice blocking and the growing process of the deposits. The growing process of deposits was kinescoped by a CCD camera, and the growing velocity were measured. At the same time, the cell voltage and time was recorded with computer. Temperature was controlled by circulators with a programmable or digital controller (Polystat).

The structure and phase composition of the electrochemically deposited formation were identified by electron diffraction analysis, bright-field imaging, dark-field imaging, and high-resolution electron microscopy image in a FEG 2000 transmission electron microscope. The surface

morphology at these experimental conditions was observed in a LEO-1550 scanning electron microscope.

3. Results and discussion

Fig. 1(a) shows the SEM morphology of typical electrodeposition with branched growth. The branch structure grows on a substrate with relatively regular branches and breaches within a two-dimensional plane. The branched structures have distinctly periodic structure along the branch with nanograins, as shown in Fig. 1(b). The fine polycrystalline features are made of carpet gains arranging

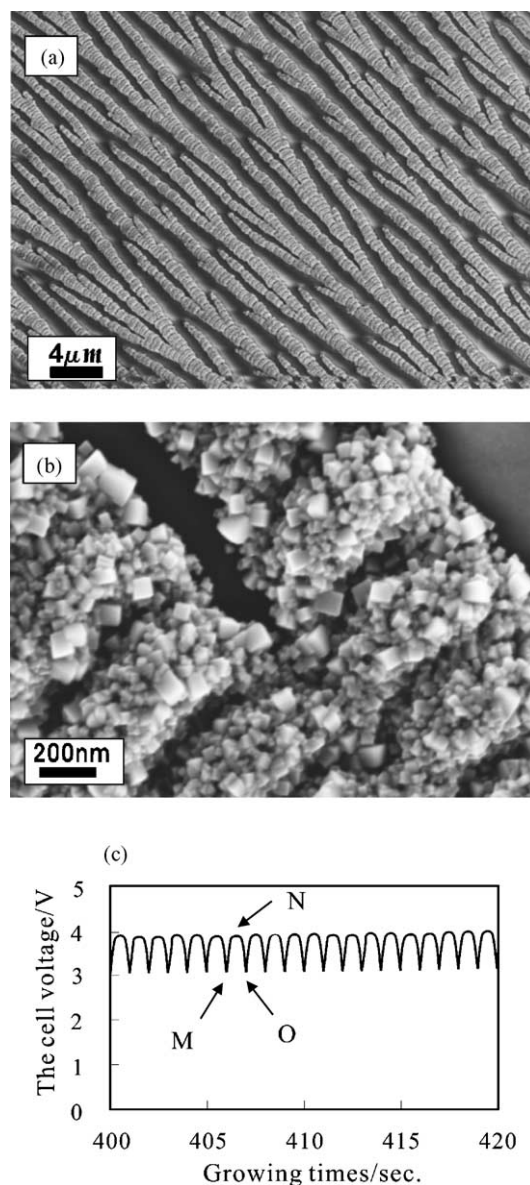


Fig. 1. (a) The SEM microstructure of typical electrodeposition with branched growth in a nanoscale ultrathin electrolyte film; (b) the depositing have a distinctly periodic structure with nanograins; and (c) the cell voltage (V) as a function of time (t), under an electrolyte CuSO_4 concentration of 0.05 M, an applied current of $30\ \mu\text{A}$ and a electrolyte pH 4.25 at $-4.5\ ^\circ\text{C}$.

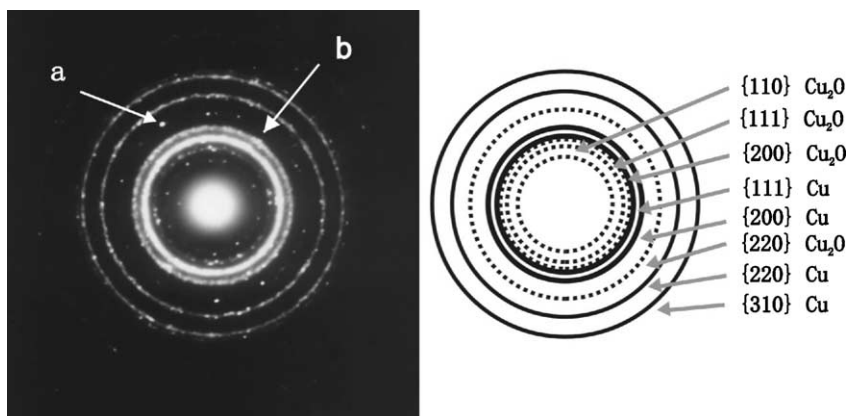


Fig. 2. TEM images and electron diffraction pattern.

side by side. The size of the nanograins is <60 nm. The TEM diffraction patterns made up of the polycrystalline diffraction ring of Cu and Cu_2O suggest the existence of Cu and polycrystalline Cu_2O (Fig. 2). Fig. 1(c) indicates a plot of the cell voltage (V) as a function of time (t), when the deposits grew on a cathode at a constant current ($30 \mu\text{A}$). It has been confirmed that the periodic structure and the periodic variations of cell voltage have a close connection by in situ observations of the growth velocity and recorded relationship between the cell voltage and time. The growth velocity is about 300 nm/s . It took 1 s for the aggregate to develop one unit. The periodicity of the cell voltage is 1 Hz . The aggregate develop one unit, and at the same time, the periodicity of the cell voltage oscillates one time.

The results illustrated above suggest that the growth process includes nucleation and growth events. The nucleation frequency is random in nature, while the growth occurs within a specified interval. The newly triggered nucleation and the size of new grain were dependent on nucleation and growth kinetics. When the driving force reaches a critical value, nucleation and growth events occur, otherwise the growth process is totally inhibited.

In the electrocrystallization process, the over-potential is the driving force, which leads to the formation of a new phase (nucleation or growth) at the electrode–electrolyte interface [26].¹ We make the assumption that the anode potential remains fixed during the process [12]. The most interesting changes in the cell voltage are due to cathode processes [12]. When a constant current ($30 \mu\text{A}$) was applied in the two poles of the cell, the cathode is charged, and the cell voltage increases. The potential of cathode becomes more negative with respect to the anode, and the cathode over-potential also

becomes more negative. At the same time, the concentration of Cu^{2+} ion was improved near cathode by the electric field effect. According to the Nernst equation, the standard electrode potential of Cu and Cu_2O is a function of the Cu^{2+} concentration. The standard electrode potential was increased by increasing the concentration of Cu^{2+} . When the cathode over-potential reaches the reaction over-potential (V_f) and the standard electrode potential reaches the standard electrode potential of reaction (the deposition potentials), the nucleation and growth events take place. The segment curve MN in Fig. 1(c) indicates the cell voltage increases by charging in the cathode, the cathode over-potential reaches the deposition potentials for Cu and Cu_2O (about 3.9 V) under the experiment condition, and the deoxidization occurs at the top of the curve. In the growth process, the cation and the charge are rapidly depleted. Therefore, the concentration of the ion close to the region of the cathode is lower than in the bulk [18]. When the transport velocity of cation is less than the deposition velocity at the growing interface, the concentration of cation decreases, pH increases, and the standard electrode potential of Cu and Cu_2O decreases. At the same time, the cathode charge is depleted; the cathode over-potential increases; and the surface field collapses. The curve segment NO in Fig. 1(c) indicates the cell voltage decrease by the surface field collapses, reduction ceases in the cathode, and new nucleation events are totally inhibited.

Since the conductivity of the electrolyte goes to zero and the current remains constant, the cathodes are charged and $V(t)$ must diverge at this time. In practice, the cell voltage increases, and the cathode over-potential is decreased. The concentration gradient becomes stronger very close to the cathode, and then diffusive transport across the depletion region becomes important. Owing to migration of cations in the once again growing interface, the concentration of Cu^{2+} increases, pH decreases, and the electrode potential is increased. A large field is formed again on the surface, up to the point when a new nucleation is fired, and the process repeats itself. As a result, the aggregate have distinct periodic structure and the cathode over-potential has a spontaneously periodic potential.

¹ In the electrocrystallization process, the electrode–electrolyte interface plays a major role [13]. At the electrode–electrolyte interface, the rate of charge transfer across the interface is an important factor. The arrangement of charges and oriented dipoles constituting the interface region at the boundary of an electrolyte is described as an electric double layer [24,25]. A potential drop also develops across the double layer at electrode surfaces. There exists the cathodic over-potential (V_g) in the double layer of the cathode [24,25].

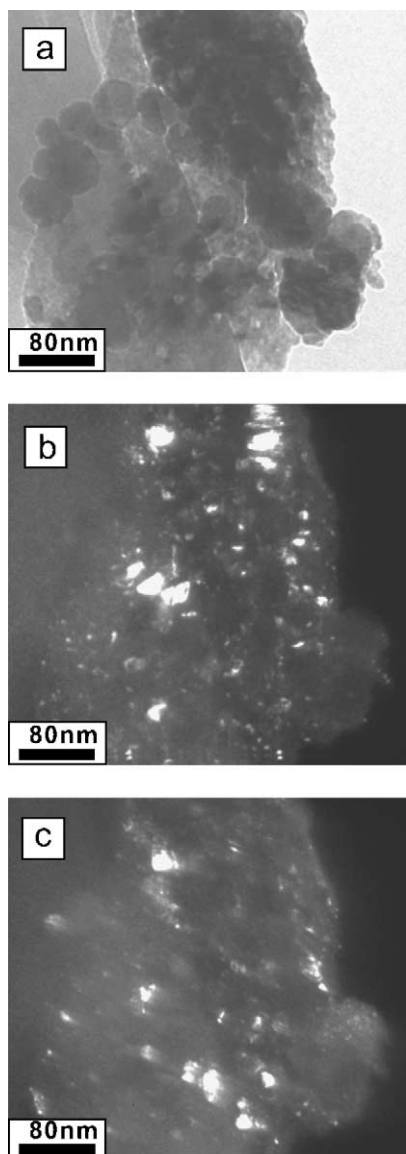


Fig. 3. Bright-field image and dark-field TEM images: (a) the bright-field image consists of nanograins; (b) the dark-field image of Cu_2O was obtained by diffraction ring of $\text{Cu}_2\text{O}(2\ 2\ 0)$ (the polycrystalline diffraction ring location a in Fig. 2); and (c) the dark-field image of Cu was obtained through the diffraction ring of $\text{Cu}(2\ 0\ 0)$ (the polycrystalline diffraction ring location b in Fig. 2).

Fig. 3 is the TEM bright-field image and dark-field image of one unit. Fig. 4 is a high-resolution electron microscopy image. The bright-field image (Fig. 3(a)) shows the morphology consisting of nanograins, while the dark-field image indicates that nanograins of Cu and Cu_2O (bright area) were scattered at a difference site, which is shown in Fig. 3(b) and (c). Figs. 3 and 4 indicate that nanograins of copper and cuprous oxide were irregular size and arrangement.

In the process of nucleation and growth, the cathode over-potential reaches the reaction over-potential; the standard electrode potential $\text{Cu}/\text{Cu}_2\text{O}$ reaches the standard electrode potential of reaction; and the nucleation of copper and cuprous oxide compete. The two electrode reactions are

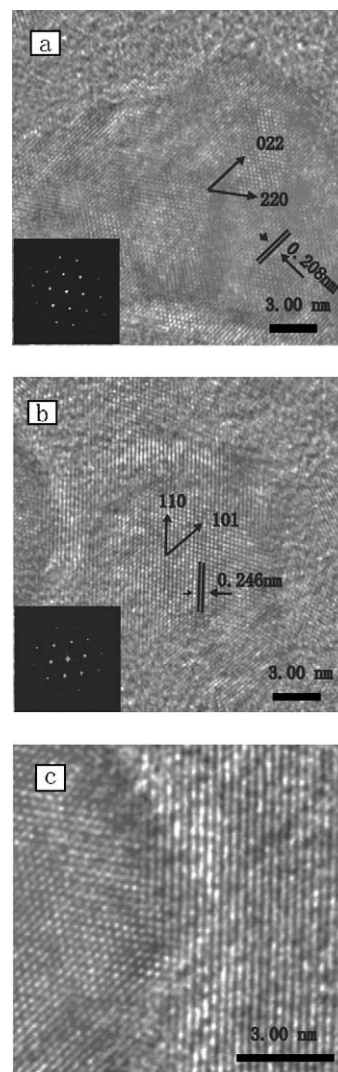
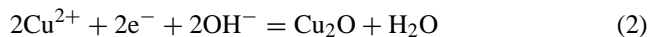


Fig. 4. High-resolution electron microscopy image (a) and (b) is the border of two grains; (a) is Cu and (b) is Cu_2O was confirmed using face interval and microdiffraction of the high-resolution electron microscopy image, and (c) the intergrains of two grains (cuprous oxide has a primitive cubic structure, with space group $Pn3m$, and a lattice parameter of 0.517 nm. Copper metal has a face-centered cubic structure, with space group $Fm3m$, and a lattice parameter of 0.427 nm).

written in Eqs. (1) and (2):



Higher nucleation rates and larger nucleation sites in the electrocrystallization process will lead to depositing with a polycrystal nature. In the growing process of each periodic structure, the equilibrium electrode potential of Cu_2O (0.17 V) is higher than that of Cu (0.34 V), so the deposition of Cu_2O is priority. According to Eq. (2), the formation of Cu_2O would deplete OH^- and Cu^{2+} in the migration layer, decreasing the local pH. The standard electrode potential of Cu_2O becomes lower than the standard electrode potential of reaction with OH^- depletion. When the nucleation of

Cu occurs, the formation of Cu would deplete Cu^{2+} in the migration layer, according to Eq. (1). The concentration of OH^- ion is refreshed again, and the standard electrode potential of Cu_2O exceeds the standard electrode potential of reaction. The above process repeats itself until the cathode over-potential gets much smaller than the reaction over-potential. The formation of $\text{Cu}/\text{Cu}_2\text{O}$ electrochemical deposition is oscillatory nucleation and growth. However, due to the crystallite capture the amount of ion is different, the formation of every crystal (Cu_2O) differ in depleting OH^- and Cu^{2+} , the crystal differ in size, they result in the front of the growing interface is irregular. In accordance, the nucleation sites of Cu crystal are too irregular. Thereby, the distribution of $\text{Cu}/\text{Cu}_2\text{O}$ nanograins is random to all appearances (see Fig. 3). A mixture of copper and cuprous oxide is deposited and grains form on the uncoated cover glass substrate from a copper sulfate solution. The changes in the local $\text{Cu}/\text{Cu}_2\text{O}$ rate are too weak for the cell potential curve to be the cause of the changes (see Fig. 1c).

4. Conclusions

In the presence of an ultrathin layer of concentrated CuSO_4 electrolyte, the depositing have a distinct periodic structure with randomly distributed $\text{Cu}/\text{Cu}_2\text{O}$ nanograins, and relatively regular branch and breach were formed on two-dimensional plane.

In the electrocrystallization process, the change of the cathode over-potential and the standard electrode potential for Cu_2O and Cu result in a periodic structure and spontaneously periodic variations of cell voltage. In the front of the growing interface, the presence of copper and cuprous oxide can be justified a competition between the two electrode reactions because the electrode potentials for Cu_2O and Cu are different. A mixture of copper and cuprous oxide is deposited as a structure with the randomly distributed $\text{Cu}/\text{Cu}_2\text{O}$ nanograins.

Acknowledgements

This work was supported by the grants from the Ministry of Science and Technology of China (No. G1998061410), the National Science Foundation of China (Nos. 19974014 and 10021001).

References

- [1] D. Edelstein, J. Heidenreich, R. Goldblatt, W. Cote, C. Uzoh, N. Lustig, et al., *Tech. Dig. Int. Electron. Devices Meet. IEEE*, Washington, DC, 1997, p. 773.
- [2] S. Venkatesan, A.V. Gelatos, V. Misra, B. Smith, R. Islam, J. Cope, et al., *Tech. Dig. Int. Electron. Devices Meet. IEEE*, Washington, DC, 1997, p. 769.
- [3] T. Vicsek, *Phys. Rev. Lett.* 53 (1984) 2281.
- [4] Y. Sawada, A. Dougherty, J.P. Gollub, *Phys. Rev. Lett.* 56 (1986) 1260.
- [5] F. Sagues, M.Q. Lopez-Salvans, J. Claret, *Phys. Rep.* 337 (2000) 97.
- [6] M.-Q. Lopez-Salvans, P.P. Trigueros, S. Vallmitjana, J. Claret, F. Sagues, *Phys. Rev. Lett.* 76 (1996) 4062.
- [7] C. Leger, L. Servant, J.L. Bruneel, F. Argoul, *Phys. A* 263 (1999) 305.
- [8] C. Leger, J. Elezgaray, F. Argoul, *Phys. Rev. E* 61 (2000) 5452.
- [9] M. Wang, W.J.P. van Enckevort, N.-B. Ming, P. Bennema, *Nature (Lond.)* 367 (1994) 438.
- [10] D. Barkey, F. Oberholtzer, Q. Wu, *Phys. Rev. Lett.* 75 (1995) 2980.
- [11] A. Kuhn, F. Argoul, J.F. Muzy, A. Arneodo, *Phys. Rev. Lett.* 73 (1994) 2998.
- [12] R. de Bruyn, *Phys. Rev. E* 56 (1997) 3326.
- [13] J.-N. Chazalviel, *Phys. Rev. A* 42 (1990) 7355.
- [14] V. Fleury, J.-N. Chazalviel, M. Rosso, B. Sapoval, *J. Electroanal. Chem.* 290 (1990) 249.
- [15] V. Fleury, J.-N. Chazalviel, M. Rosso, *Phys. Rev. Lett.* 68 (1992) 2492.
- [16] J.-N. Chazalviel, M. Rosso, E. Chassaing, V. Fleury, *J. Electroanal. Chem.* 407 (1996) 61.
- [17] A. Kuhn, F. Argoul, *Phys. Rev. E* 49 (1994) 4298; A. Kuhn, F. Argoul, *J. Electroanal. Chem.* 371 (1994) 93.
- [18] F. Argoul, E. Freysz, A. Kuhn, C. Leger, L. Potin, *Phys. Rev. E* 53 (1996) 1777.
- [19] V. Fleury, *Nature* 390 (1997) 145.
- [20] V. Fleury, W.A. Watters, L. Allam, T. Devers, *Nature* 416 (2002) 716.
- [21] V. Fleury, D. Barkey, *Phys. A* 233 (1996) 730.
- [22] M. Wang, S. Zhong, X.-B. Yin, J.-M. Zhu, R.-W. Peng, N.-B. Min, *Phys. Rev. Lett.* 86 (2001) 3827.
- [23] S. Zhong, M. Wang, X.-B. Yin, J.-M. Zhu, R.-W. Peng, N.-B. Min, *J. Phys. Soc. Japan* 70 (2001) 1452.
- [24] J. Dini, *Electrodeposition*, Noyes, New Jersey, 1992.
- [25] P. Ramasany, in: C.J. Hurlle (Ed.), *Handbook of Crystal Growth 1a*, North-Holland, Amsterdam, 1993.
- [26] E. Budevski, G. Staikov, W.J. Lorentz, *Electrochemical Phase Formation and Growth an Introduction to the Initial Stages of Metal Deposition*, VCH, New York, 1996 (Chapter 4.5).
- [27] K.J. Vetter, *Electrochemical Kinetics—Theoretical Aspects*, Section D, Academic Press, New York, 1967, Chapter 2, p. 282.
- [28] J.A. Switzer, C.-J. Hung, L.-Y. Huang, F.S. Miller, Y.-C. Zhou, E.R. Raub, et al., *J. Mater. Res.* 13 (1998) 909.
- [29] E.W. Bohannon, L.-Y. Huang, F.S. Miller, M.G. Shumsky, J.A. Switzer, *Langmuir* 15 (1999) 813.